

Hydrogel formation by photocrosslinking of dimethylmaleimide functionalized polyacrylamide

Sebastian Seiffert^a, Wilhelm Oppermann^{a,*}, Kay Saalwächter^b

^a Institute of Physical Chemistry, Clausthal University of Technology, Arnold-Sommerfeld-Strasse 4, D-38678 Clausthal-Zellerfeld, Germany

^b Institute of Physics, Martin-Luther-University Halle-Wittenberg, Friedemann-Bach-Platz 6, D-06108 Halle, Germany

Received 21 May 2007; received in revised form 4 July 2007; accepted 5 July 2007

Available online 14 July 2007

Abstract

Polyacrylamide (PAAm) hydrogels are obtained in an efficient and controlled manner by means of photocrosslinking of linear PAAm chains which are functionalized with dimethylmaleimide (DMMI) groups. The reaction is conveniently performed in the presence of thioxanthone disulfonate as a triplet sensitizer.

The fundamental investigation of the photoreaction on the basis of model compounds shows that the dimerization of DMMI groups in aqueous solution leads to asymmetric products instead of the expected cyclobutane derivatives. Nevertheless, crosslinking occurs in a well controlled manner without perceptible side reactions. The systematic analysis of the progress of the reaction by means of UV–vis spectroscopy indicates that the rate of dimerization is simply proportional to the concentration of sensitizer and the intensity of irradiation. The dimerization reaction can be interrupted at any intermediate stage by discontinuing the UV irradiation in order to study the system as it changes from a semi-dilute polymer solution to a fully crosslinked gel.

The network formation was investigated macroscopically by rheology and microscopically by multiple-quantum NMR experiments. The results clearly indicate that the formation of active network strands occurs in proportion with DMMI conversion. The crosslinking efficiency varies markedly with concentration, but is surprisingly high (>60% at 80 g L⁻¹), while the length of the network chains seems to be independent of concentration.

© 2007 Elsevier Ltd. All rights reserved.

Keywords: Polyacrylamide; Dimethylmaleimide; Photocrosslinking

1. Introduction

Hydrogels formed by crosslinking of water-soluble polymers have gained increasing importance during the last decades. They provide the basis for a variety of applications in fields like super-absorbent polymer technology, chromatography, or electrophoresis. Moreover, their potential in biophysics and nanotechnology, e.g., for controlled drug release or enzyme treatment, is still being explored.

One of the most important non-ionic, water-soluble synthetic polymers for the preparation of crosslinked structures

is polyacrylamide (PAAm) [1–4]. The usual way to build-up PAAm networks is the free radical crosslinking copolymerization of acrylamide with *N,N'*-methylendiacylamide or another suitable crosslinker [1,5]. However, the so-obtained networks often turn out to be relatively inhomogeneous [6–8]. An alternative for PAAm network formation could be to start out from semi-dilute solutions of well-defined functionalized linear PAAm molecules, which are subsequently crosslinked by selectively connecting the functional groups. It is an advantage of the latter method that in this case the crosslinking occurs in a random manner and, moreover, that the properties of the physically entangled system and the chemically crosslinked network structure can be consistently compared.

Achieving the crosslinking of existent linear polymer chains through a photochemical reaction offers a convenient

* Corresponding author. Tel.: +49 5323 72 2205; fax: +49 5323 72 2863.

E-mail address: wilhelm.oppermann@tu-clausthal.de (W. Oppermann).

feature in this respect: the reaction is readily controlled by adjusting the irradiation conditions, and its progress can be stopped, if desired, by interrupting the light exposure. The system can thus be studied and characterized at any intermediate stage on its path from sol to gel, before resuming the irradiation.

In this work, use of the photochemical [2 + 2] dimerization of dimethylmaleimide (DMMI) side groups was made as sketched in Fig. 1. A sensitizer, thioxanthone disulfonate, was employed to enable the photoreaction by irradiation with long-wave UV light. Although photochemical crosslinking reactions have been utilized several times to prepare various types of swollen hydrogels [9–13], there are no reports on a detailed and fundamental examination of the reaction mechanism when pendent DMMI groups are used to crosslink PAAm, and on the development of the network structure in such systems. The aim of the present study is therefore to provide such fundamental knowledge. First, the DMMI dimerization reaction in aqueous solution is studied on low molecular weight model compounds. Then, we investigate the kinetics of the gelation process when PAAm hydrogels are formed by means of DMMI side group dimerization, focusing in particular on the possibilities for monitoring and controlling the progress of the reaction. Finally, rheological measurements and multiple-quantum NMR experiments provide information on the network structures on a macroscopic and a microscopic

scale, respectively. They indicate that the hydrogels thus obtained are formed in a very efficient and controlled way.

2. Theoretical background and strategy for the present work

Suitable groups which undergo photodimerization and can therefore be used for photocrosslinking of accordingly functionalized polymers comprise cinnamate (and related) moieties [14–27], coumarins [28–33], and maleic acid derivatives like dimethylmaleimide (DMMI) [34–49]. One of the major drawbacks of cinnamates, besides advantageous features such as controlled reversibility of the dimerization [22], is the photochemically induced *cis/trans* isomerization resulting in a noticeable decrease of the quantum yield of photocrosslinking [39]. A second shortcoming is their susceptibility to radical reactions, which precludes them from being used in radical copolymerizations. Coumarins and DMMIs do not show these disadvantages. We chose to employ DMMI-functionalized PAAm because of the higher polarity and water solubility of this group, and because of favorable spectroscopic and electronic properties.

Photochemical [2 + 2]-cycloaddition reactions can principally start from both the excited singlet (S_1) and the triplet (T_1) states of one of the two molecules eventually forming the dimer. In the first case, the reaction occurs in a concerted action, originating from a *syn* exciplex that is stabilized by secondary orbital interactions and yields cyclodimers in the stereospecific *cis* form. The reaction from the T_1 state, on the other hand, proceeds in a stepwise manner. Starting from a triplet-exciplex having a long lifetime, the addition occurs via an intermediate 1,4-diradical with wide geometry that finally relaxes to the ground state (S_0), where the second bond is formed. Dimeric products thus obtained are a mixture of *cis* and (favored) *trans* isomers.

The energy of the excited singlet state of DMMI is considerably higher than that of the triplet state. Direct excitation of DMMI requires short-wave UV light which might as well cause unwanted degradation of the polymer chains. It is therefore advantageous to proceed from the T_1 state, which can be reached by energy transfer from an excited, suitably chosen sensitizer. The S_1 and T_1 states of the sensitizer molecule have to be closer together with their energies between those of the S_1 and the T_1 states of DMMI. Fig. 2a shows a scheme of such a sensitized process. After excitation of the sensitizer to its S_1 state by comparatively long-wave UV light, it can undergo intersystem crossing to its slightly lower T_1 state and subsequently transfer the triplet energy to the substrate (DMMI), from which the dimerization reactions proceed. This way of effectively achieving a high population of the T_1 state as a starting point for photochemical reactions was described by Hammond et al. [50–54]. Suitable sensitizer molecules are aromatic ketones since they generally show a combination of strong spin-orbit coupling, leading to high quantum yield of intersystem crossing, and small energy gaps between the S_1 and the T_1 states. In addition, their $n\pi^*$ or $\pi\pi^*$ triplet states provide sufficiently high energy levels

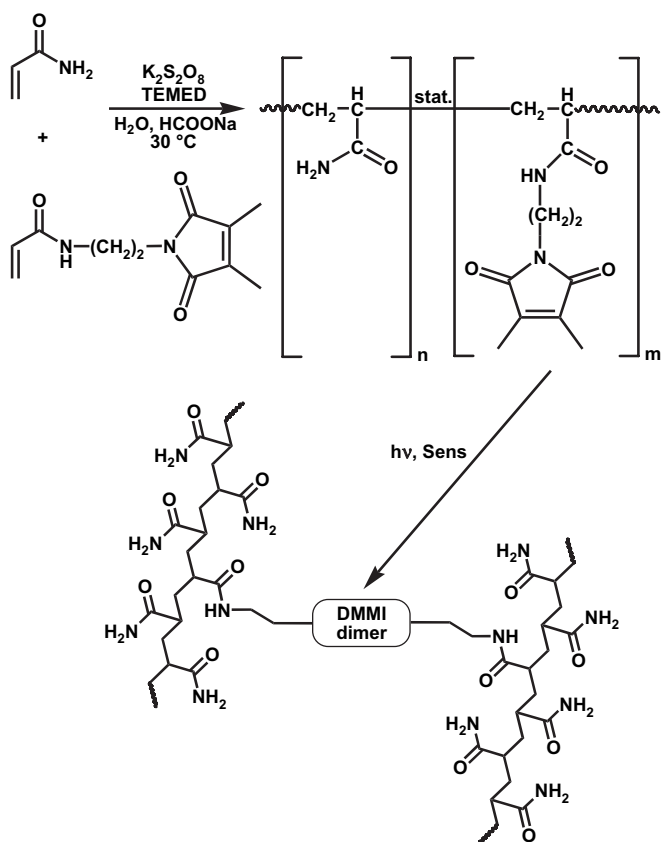


Fig. 1. Scheme of the copolymerization of acrylamide (AAm) with *N*-(*N'*-acryloyl-2-aminoethyl)-dimethylmaleimide (DMMIAAm) and illustration of the sensitized photocrosslinking of the copolymer.

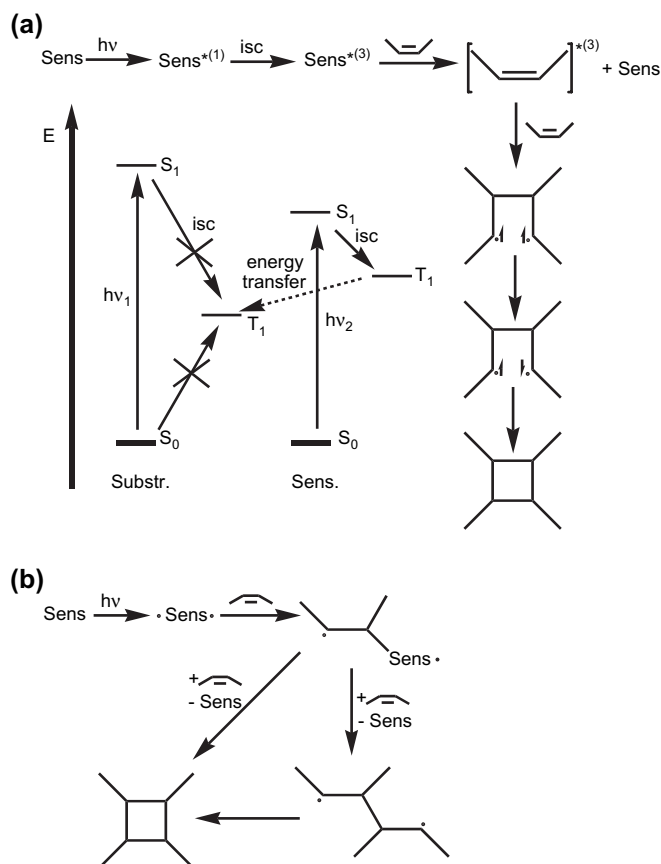


Fig. 2. Mechanism of sensitized [2+2]-cycloaddition according to (a) Hammond et al. [50–54] and (b) Schenck et al. [53,56].

and lifetimes [55] to enable effective energy transfer to a substrate.

A slightly different mechanism of sensitized photoreactions was suggested by Schenck et al. [53,56], who assumed formation of an intermediate adduct between sensitizer and substrate as depicted in Fig. 2b.

The majority of aromatic ketones possesses $n\pi^*$ triplet states. These molecules can undergo various types of side reactions such as hydrogen abstractions or Paterno-Büchi additions [57,58]. Molecules with $\pi\pi^*$ triplet states are therefore preferred as sensitizers, because unwanted reactions can be largely excluded. There have been several studies showing that the T_1 state of thioxanthenes in polar media corresponds to a $\pi\pi^*$ transition [59,60]. Thioxanthenes have been widely used for photosensitization and initiation purposes [61,62]. The energy of their T_1 state is relatively high [50,63] and only marginally less than that of S_1 . Intersystem crossing occurs with high quantum yield [63–65], and they show adequately long triplet lifetimes [59]. In the present work, we employed the sodium salt of thioxanthone disulfonate. The sulfonate groups only act in terms of increasing the water solubility without affecting the spectral properties significantly [59,66].

Besides allowing for mild irradiation conditions by shifting the excitation towards longer wavelengths, the usage of a sensitizer has the second advantage that the concentrations of the

light absorbing species and of the reacting species can be adjusted independently. This is necessary in order to keep the absorbance in the utilized wavelength range small enough to ensure constant irradiation conditions over the whole reaction vessel, particularly when big, yet spatially homogeneous samples are to be prepared.

3. Experimental

3.1. Materials

3.1.1. *N*-(2-Hydroxyethyl)-dimethylmaleimide (HE-DMMI)

HE-DMMI was synthesized in similar manner as described in Ref. [39] by heating a solution of 75 mmol 2-aminoethanol (Aldrich) and 75 mmol dimethylmaleic anhydride (Aldrich) in 200 mL toluene (Aldrich) for 2 h at 120 °C on a water trap. After removing the solvent, the crude product was purified by solid-state distillation at 110 °C/0.05 mbar with a cooling water temperature of about 70 °C to give HE-DMMI as a whitish solid in quantitative yield that was characterized by ^1H and ^{13}C NMR spectroscopies.

^1H NMR (400 MHz, CDCl_3): δ = 1.97 (s, 6H, 2 CH_3), 2.78 (br, 1H, OH), 3.61–3.81 (m, 4H, $\text{HO}-(\text{CH}_2)_2$ -DMMI) ppm.

^{13}C NMR (100 MHz, CDCl_3): δ = 8.7 (CH_3), 40.8 ($\text{HO}-\text{CH}_2-\text{CH}_2$ -DMMI), 61.2 ($\text{HO}-\text{CH}_2-\text{CH}_2$ -DMMI), 137.4 ($\text{C}=\text{C}$), 172.6 ($\text{C}=\text{O}$) ppm.

3.1.2. *N*-(*N*'-Acetyl-2-aminoethyl)-dimethylmaleimide

A solution of 8 mmol *N*-acetyl-2-diaminoethane (Lancaster, purified by solid-state distillation at 70 °C/0.1 mbar with a cooling water temperature of about 50 °C) and 8 mmol dimethylmaleic anhydride (Aldrich) in 50 mL toluene (Aldrich) was heated for 3 h at 120 °C on a water trap. After removing the solvent, the crude product was purified by recrystallization from hexane/ethyl acetate (1:1) to give *N*-(*N*'-acetyl-2-aminoethyl)-dimethylmaleimide as a whitish solid in quantitative yield that was characterized by ^1H and ^{13}C NMR spectroscopies.

^1H NMR (400 MHz, $\text{DMSO}-d_6$): δ = 1.72 (s, 3H, $\text{H}_3\text{C}-\text{CONH}$), 1.89 (s, 6H, $\text{H}_3\text{C}-\text{C}=\text{C}-\text{CH}_3$), 3.15 (dt, $^3J = 6.1$ Hz, 2H, $\text{CONH}-\text{CH}_2-\text{CH}_2$ -DMMI), 3.41 (t, $^3J = 6.0$ Hz, 2H, $\text{CONH}-\text{CH}_2-\text{CH}_2$ -DMMI), 7.92 (t, $^3J = 5.8$ Hz, 1H, CONH) ppm.

^{13}C NMR (100 MHz, $\text{DMSO}-d_6$): δ = 8.5 ($\text{C}=\text{C}-\text{CH}_3$), 22.5 (CH_3-CONH), 36.9 ($\text{CONH}-\text{CH}_2-\text{CH}_2$ -DMMI), 37.3 ($\text{CONH}-\text{CH}_2-\text{CH}_2$ -DMMI), 136.6 ($\text{C}=\text{C}$), 169.4 (CH_3-CONH), 171.7 (ring $\text{C}=\text{O}$) ppm.

3.1.3. Sodium thioxanthone-2,7-disulfonate (TXS)

TXS as introduced by Gupta et al. [67] was chosen as water-soluble triplet sensitizer. Its properties have been studied by Kronfeld and Timpe [59], whose approach for synthesis and characterization was followed here. The product was obtained as a mixture with Na_2SO_4 containing about 4 wt.% TXS (sodium salt).

3.1.4. *N*-(*N'*-Acryloyl-2-aminoethyl)-dimethylmaleimide (DMMIAAm)

Synthesis of DMMI-functionalized acrylamide (DMMIAAm) [44] was performed essentially according to Ref. [46]: one amine group of 2-diaminoethane (Fluka) was blocked with Boc (Fluka), the other one was then reacted with dimethylmaleic anhydride (Aldrich), and, after removing the protecting group, the amine group was reacted with acryloyl chloride (Merck). The following purification steps for the intermediate compounds and the final product were applied: BocNH-(CH₂)₂-NH₂ was purified by vacuum distillation at 58 °C/0.1 mbar, BocNH-(CH₂)₂-DMMI was recrystallized from water/ethanol (1:1), H₂N-(CH₂)₂-DMMI was intensively washed with methylene chloride and DMMIAAm was purified by recrystallization from hexane/ethyl acetate (1:1).

3.1.5. Poly(AAm-co-DMMIAAm)

Four high molecular weight samples of P(AAm-co-DMMIAAm), herein abbreviated as PAAm-DMMI, with varying amounts of DMMI moieties ranging from 0.7 to 2 mol% were prepared by free radical copolymerization as depicted in Fig. 1 in the following manner adopted from Ref. [68].

An aqueous solution of 800 mL containing a total of 368 mmol of the monomers acrylamide (Merck) and DMMIAAm in the ratios summarized in Table 1 as well as 11.5 mmol of sodium formate (Fluka) as a chain transfer agent [68,69] was flushed with nitrogen for about 10 min at 30 °C. The polymerization was initiated by the addition of 0.1 mol% (relating to the total amount of monomers) of potassium peroxydisulfate (Aldrich) and 0.25 mol% of *N,N,N',N'*-tetramethylethylenediamine (TEMED, Fluka) in the form of small amounts of appropriately concentrated aqueous solutions. Several mechanisms of decomposition of the initiator/accelerator system are discussed in the literature [70,71]. While the reaction was running at 30 °C under nitrogen atmosphere, aliquots were withdrawn from the mixture and dropped into an excess of methanol in order to check for precipitation. This was done every minute in the beginning and at longer intervals later. When a perceptible precipitation was noticed, the reaction was interrupted by precipitation into a 10-fold excess of methanol containing about 2 wt.% of concentrated hydrochloric acid. Conversions achieved by this procedure were about 5% in all cases treated in this work. The corresponding reaction times

are listed in Table 1. The crude product was isolated by filtration, washed with methanol, redissolved in water, and dialyzed against water for about 10 days. Finally, the purified polymer was isolated by freeze-drying. The obtained copolymers were characterized by ¹H NMR spectroscopy.

¹H NMR (400 MHz, D₂O): δ = 0.80–2.60 (br, xH, all backbone protons + DMMI methyl protons), 3.00–3.70 (br, 4H, CONH-(CH₂)₂-DMMI) ppm.

The compositions of the copolymers were estimated from the integrals of the corresponding NMR signals. Setting the integral of the broad signal at 3.00–3.70 ppm to 4, the mole ratio of AAm and DMMIAAm groups in the copolymer is obtained from the integral *x* of the broad high field NMR signal (0.8–2.6 ppm) in the following manner: *x* was first reduced by 9 (3 backbone protons plus 6 methyl protons in each DMMIAAm residue) and afterwards divided by 3 (3 protons per acrylamide residue). The resulting number is the ratio AAm/DMMIAAm in the copolymer. Table 1 summarizes the results for the four prepared samples discussed in this work. Also compiled in Table 1 are the molecular weights obtained via SEC and measurements of intrinsic viscosity. The fact that they decrease with increasing DMMIAAm fraction indicates that DMMIAAm might act as a controlling agent here (q.v., [45]).

3.2. Characterization

UV–vis absorption spectra were obtained on a Jasco V-550 spectrometer.

High resolution ¹H and ¹³C NMR spectra were recorded on a Bruker Avance 400 digital FT spectrometer at 400 and 100 MHz, respectively. Chemical shifts are reported in ppm relative to internal tetramethylsilane (δ = 0.00 ppm) for organic solvents and relative to internal H₂O (δ = 4.79 ppm [72]) when D₂O was used as the solvent. Abbreviations: s = singlet, d = doublet, t = triplet, q = quartet, m = multiplet, br = broad.

Mass spectra were recorded on a Hewlett–Packard HP5989 MS engine with 70 eV electronic ionization.

SEC measurements were performed commercially by Polymer Standards Service GmbH (PSS Mainz, Germany) utilizing PSS Suprema columns with an eluent composed of 0.1 mol L⁻¹ NaCl/0.1 vol.% TFAc. Calibration was performed with pullulan standards. Hence, molecular weights are obtained as apparent pullulan equivalent values.

Table 1
Compositions of reaction mixtures for copolymerizations of AAm with DMMIAAm, as well as characteristic data of the obtained low-conversion products

Name of sample	Composition of the reaction mixture			Characterization of the resulting low-conversion products						
	AAm (mol%)	DMMIAAm (mol%)	Reaction time ^a (min)	Integral <i>x</i> in ¹ H NMR (rel. number of protons)	DMMIAAm fraction in the copolymer (mol%)	<i>M</i> _N ^b (g mol ⁻¹)	<i>M</i> _w ^b (g mol ⁻¹)	<i>M</i> _w / <i>M</i> _N	[η] (mL g ⁻¹)	<i>M</i> _n ^b (g mol ⁻¹)
PAAm-DMMI1.0	99.0	1.0	35	428.71	0.71	361 500	920 000	2.55	245.175	640 000
PAAm-DMMI1.5	98.5	1.5	60	275.78	1.11	301 000	775 500	2.58	198.390	480 000
PAAm-DMMI2.0	98.0	2.0	50	201.75	1.53	241 500	574 500	2.38	192.190	460 000
PAAm-DMMI2.5	97.5	2.5	75	158.97	1.96	207 500	531 000	2.56	162.726	370 000

^a Reaction times were adjusted to give conversions of about 5% in each case.

^b Molecular weights were obtained as apparent pullulan equivalent values by SEC, as well as viscosity averages from the intrinsic viscosities in solutions of 0.5 mol L⁻¹ NaCl at 20 °C employing Mark–Houwink–Sakurada parameters as reported by McCarthy et al. [73].

Measurements of solution viscometry were made on polymer solutions with concentrations of 0.5, 1, 1.5 and 2 g L^{-1} at 25°C using an Ubbelohde viscometer with a capillary diameter of 0.36 mm. The solvent employed was an aqueous solution of 0.5 mol L^{-1} NaCl in each case. Intrinsic viscosities were estimated with the aid of Huggins plots. For calculation of the viscosity average molecular weight, Mark–Houwink–Sakurada parameters reported by McCarthy et al. [73] were used.

3.3. Irradiation conditions

The light source employed in most of the photochemical dimerization and crosslinking reactions was a 100 W xenon short arc lamp (Osram XBO), providing a broad and relatively unstructured spectrum in the range of 200–500 nm. By using two different optical filters, suitable wavelength ranges were selected: a broad-band pass filter of type BG25 (Reichmann Feinoptik GmbH, Brokdorf, Germany) enabled the efficient excitation of the thioxanthone sensitizer while simultaneously blocking UV light with $\lambda < 310 \text{ nm}$, while a narrow-band interference filter of type 380FS10-50 (LOT Oriel, Darmstadt, Germany) was chosen for selective excitation at $(383 \pm 5.6) \text{ nm}$ when high intensity was not necessary or appropriate. Fig. 3 shows the UV–vis absorption spectra of HE-DMMI and of TXS in water together with the transmittance curves of the two filters. Irrespective of which filter is employed, there is overlap only with the long-wave absorption band of TXS. This choice of conditions ensures that the DMMI moieties cannot be excited directly, but only via energy transfer from the TXS sensitizer.

3.4. Model reactions

An aqueous solution of 50 mL containing 8 mmol L^{-1} of HE-DMMI and 0.08 mmol L^{-1} of TXS was irradiated through the band pass filter BG25 in a 100 mL round-bottomed flask for about 45 h. Thereby, the formation of a small amount of a white precipitate was observed. At several intervals during

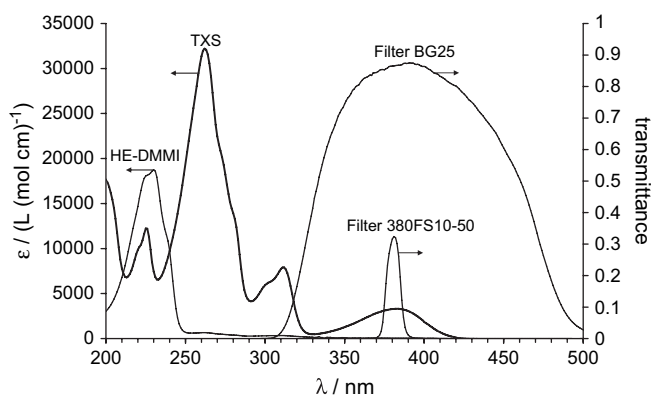


Fig. 3. UV–vis spectra of *N*-(2-hydroxyethyl)-dimethylmaleimide (HE-DMMI) and sodium thioxanthone disulfonate (TXS) in water as well as transmittances of the optical filters used in mechanistic and kinetic investigations of the PAAm–DMMI crosslinking.

irradiation, aliquots were withdrawn via syringe and analyzed by UV–vis spectroscopy using quartz cuvettes with a layer thickness of 0.1 mm (Hellma). When no further conversion was detected (after 45 h), the irradiation was stopped. The precipitate was isolated by filtration to yield about 5 mg of a white solid, while approximately 95 mg of a second whitish solid was obtained by vacuum evaporation of the solvent from the filtrate. (Note that part of this solid is Na_2SO_4 contained in the sensitizer.) Both products were characterized without further purification by ^1H and ^{13}C NMR spectroscopies in D_2O (originally dissolved product) and $\text{DMSO-}d_6$ (precipitate) as well as by mass spectrometry.

3.4.1. Precipitated product

^1H NMR (400 MHz, $\text{DMSO-}d_6$): $\delta = 1.09$ (s, 12H, 4CH_3), 3.51–3.62 (m, 8H, $2(\text{HO}-(\text{CH}_2)_2-\text{N})$), 4.93 (t, $^3J = 5.2 \text{ Hz}$, 2H, 2OH) ppm.

^{13}C NMR (100 MHz, $\text{DMSO-}d_6$): $\delta = 12.1$ (CH_3), 41.1 (CH_2-N), 48.7 (cyclobutane–C), 56.8 (CH_2-OH), 177.7 ($\text{C}=\text{O}$) ppm.

m/z (EI) = 338 ($[\text{M}]^+$, 23).

3.4.2. Dissolved product

^1H NMR (400 MHz, D_2O): $\delta = 1.19$ (d, $^3J = 7.4 \text{ Hz}$, 3H, upper CH_3 in right ring in Fig. 5b), 1.34 (s, 3H, CH_3), 1.50 (s, 3H, CH_3), 3.12 (q, $^3J = 6.8 \text{ Hz}$, 1H, methine H in right ring in Fig. 5b), 3.54–3.63 (m, 4H, $\text{HO}-(\text{CH}_2)_2-\text{N}$ in right ring in Fig. 5b), 3.69–3.75 (m, 4H, $\text{HO}-(\text{CH}_2)_2-\text{N}$ in left ring in Fig. 5b), 6.05 (d, $^2J = 0.7 \text{ Hz}$, 1H, olefinic), 6.43 (d, $^2J = 0.7 \text{ Hz}$, 1H, olefinic) ppm.

^{13}C NMR (100 MHz, D_2O): $\delta = 11.1$ (upper CH_3 in right ring in Fig. 5b), 14.9 (lower CH_3 in right ring in Fig. 5b), 17.5 (CH_3 in left ring in Fig. 5b), 40.9 (CH_2-N), 50.1 (left C of ring linkage in Fig. 5b), 50.9 (right C of ring linkage in Fig. 5b), 58.0 ($\text{OH}-\text{CH}_2$), 124.7 ($\text{C}=\text{CH}_2$), 139.2 ($\text{C}=\text{CH}_2$), 170.8 (upper $\text{C}=\text{O}$ in left ring in Fig. 5b), 179.7 (lower $\text{C}=\text{O}$ in right ring in Fig. 5b), 181.5 (upper $\text{C}=\text{O}$ in right ring in Fig. 5b), 182.0 (lower $\text{C}=\text{O}$ in left ring in Fig. 5b) ppm.

m/z (EI) = 338 ($[\text{M}]^+$, 7).

A similar experiment was performed in the presence of 8 mmol L^{-1} acetamide serving as a model compound for polyacrylamide. Also, dimerizations of *N*-(2-aminoethyl)-dimethylmaleimide and of *N*-(*N*-acetyl-2-aminoethyl)-dimethylmaleimide were carried out using similar conditions.

3.5. Photoinduced crosslinking

To study the kinetics of the crosslinking reaction, aqueous solutions containing 50 g L^{-1} of PAAm–DMMI1.5 and a variable amount of sensitizer were irradiated in quartz cuvettes of thickness 0.1 mm. The amount of TXS was adjusted to be 1–100% relating to the concentration of DMMI chromophores. UV spectra were recorded at suitable intervals. For the irradiation experiments, a set-up mounted on an optical bench was used to ensure high reproducibility of the arrangement and

spacing of light source, filter(s) and specimen. The light intensity was checked frequently during the test series by measurement with a photodiode. Two series of measurements were conducted using either of the two optical filters specified above.

In another test series, the influence of light intensity on the reaction kinetics was analyzed. Attenuation of intensity was achieved by using cascades of the filter 380FS10-50 plus a varying number of additional BG25 filters. Relative intensities of 100% ($83.0 \pm 0.8\%$), ($69.5 \pm 1.3\%$), and ($58.2 \pm 1.5\%$) could be adjusted in the wavelength range of (383 ± 5.6) nm, with 100% corresponding to about 0.1 mW cm^{-2} . The concentration of PAAm–DMMI1.5 was 50 g L^{-1} and an equimolar amount of TXS relating to that of DMMI moieties was used in this case.

As characteristic values, the half-lives of DMMI conversion were determined from the UV spectra as described in Section 4.2.1, and their dependencies on light dose and concentration of sensitizer were examined.

3.6. Rheology under UV exposure

Oscillatory measurements of the elastic modulus G' as a function of preceding crosslinking were performed on a Physica MCR500 plate–plate rheometer (plate diameter 8 mm) equipped with a measurement cell of type P-PTD-UV featuring a UV-transparent lower plate, under which a light guide was positioned. Hence, irradiation of the sample was possible during a running measurement, and the rise of the elastic modulus with progressive DMMI dimerization could be determined. As a UV source, an EXFO Novacure 2100 mercury arc lamp was employed, producing a high irradiation intensity of about 15 mW cm^{-2} at the sample position. Specimens were aqueous semi-dilute solutions of PAAm–DMMI2.0 with concentrations of 20, 40, 60 and 80 g L^{-1} . The amount of TXS was 1 mmol L^{-1} in each case.

Measurements were performed at 25°C at a frequency of 4 Hz and shear amplitude of 0.5%, which was small enough to ensure linear viscoelastic behavior. The layer thickness (plate–plate distance) was 0.1 mm. The following protocol was used to establish a reproducible sample history:

1. annealing at 25°C for 30 s,
2. shearing at constant rate for 2 s (to break inner structures, i.a.),
3. annealing without deformation for 300 s (to allow for structural recovery, i.a.),
4. oscillation without UV exposure for 30 s,
5. oscillation under UV irradiation for 300 s,
6. oscillation without UV exposure for 30 s.

To quantify the conversion of DMMI with time at these intense illumination conditions, samples of the 60 g L^{-1} solution were placed in 0.1 mm quartz cuvettes and irradiated on the same set-up for 0, 20, 55, 110, and 240 s. DMMI conversion was estimated by analyzing the corresponding UV spectra as described further below (see Section 4.2.1).

3.7. Proton multiple-quantum NMR

^1H MQ NMR measurements were performed on a Bruker minispec mp20 with $B_0 = 0.5 \text{ T}$ at 25°C . The adjustment procedures and pulse sequences applied are specified in Refs. [74–76]. For this study, 90° pulses were set to $1.7 \mu\text{s}$ and 64 scans were recorded on each sample. Specimens were fully crosslinked samples of PAAm–DMMI1.0 at concentrations of 20, 40, 60, and 80 g L^{-1} in D_2O in 10 mm OD NMR tubes. The filling height was limited to 7 mm to ensure sufficient field homogeneity over the whole sample when placed in the centre of the rf coil. The samples had been crosslinked by irradiating them for 32 h in front of a 6 W laboratory UV lamp of type NU-6K1 (Konrad Benda Laborgeräte u. Ultraviolettstrahler, Wiesloch, Germany) providing spatially homogeneous illumination in the spectral range of (365 ± 20) nm. Irradiation intensity was about 0.5 mW cm^{-2} . The long irradiation time was necessary to achieve complete reaction, since the samples contained only $10 \mu\text{mol L}^{-1}$ of TXS to ensure a transmittance of $>90\%$ at 383 nm, thus avoiding the build-up of a gradient of crosslink density across the tube. Complete conversion of the crosslinking process was verified by UV–vis measurements on aliquots of the test solutions that were placed in 0.1 mm cuvettes and irradiated parallel to the NMR tubes.

4. Results and discussion

4.1. Photoinduced dimerization of DMMI in aqueous solution

The photoinduced dimerization of DMMI in an aqueous medium was studied using *N*-(2-hydroxyethyl)-dimethylmaleimide (HE-DMMI) as a simple water-soluble model compound. Thioxanthone disulfonate (TXS) was employed as a photosensitizer. The concentration of HE-DMMI was chosen to match the one typically present in polymeric systems, e.g., in a 50 g L^{-1} semi-dilute solution of a PAAm–DMMI having a degree of functionalization of about 1 mol%. The progress of the reaction was followed by UV–vis spectroscopy. Spectra depicted in Fig. 4 show that the absorption band of the monomeric HE-DMMI at around 230 nm decreases significantly with irradiation time, while another band appears at 205 nm which must be due to the dimeric product. All spectra intercept in isosbestic points at 209, 246, and 261 nm. This means that the spectra measured during the experiment are linear combinations of the spectra of the pure monomeric and dimeric compounds, and that the extent of conversion can be deduced from them.

Former studies on this reaction in organic media performed by Schenck et al. [28] and Zweifel [39] revealed that the dimeric product is the symmetric cyclobutane derivative in *trans* form, suggesting that a triplet intermediate occurs according to the Hammond mechanism. This mechanism was also discussed for comparable maleimide dimerizations [43,66] as well as for dimerizations of dimethylmaleic anhydride [77].

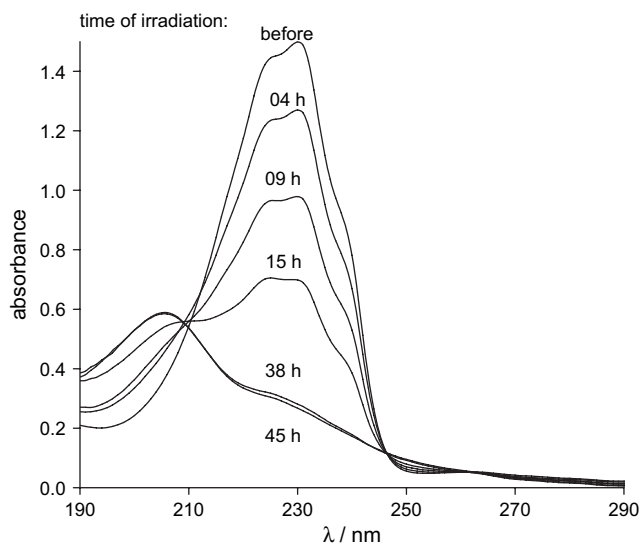


Fig. 4. UV-vis spectra taken at different reaction times to monitor the progress of the DMMI dimerization in an aqueous solution of 8 mmol L^{-1} HE-DMMI sensitized by 0.08 mmol L^{-1} TXS.

In our dimerization experiment in an aqueous system, two products could be distinguished. One minor compound appeared as a white precipitate during the reaction, while the other major one was isolated from the solution. NMR analyses of these two compounds (results given in 3.4) clearly show that they are different. The structures derived from the NMR spectra correspond to isomeric forms of a HE-DMMI dimer, which are depicted in Fig. 5. The symmetric cyclobutane derivative (Fig. 5a), which is the sole product when the photodimerization is carried out in organic solvents, is only formed as a byproduct in aqueous solution, while the major product is the asymmetric dimer shown in Fig. 5b. Formation of the latter compound requires the shift of a hydrogen atom at an intermediate reaction stage. Its structure is clearly proven by the signals at 3.12 ppm (methine hydrogen) and at 6.05 and 6.43 ppm (olefinic hydrogens) in proton NMR as well as by the signals at 124.7 and 139.2 ppm (olefinic carbons) in ^{13}C NMR. No indication for residual educt was found in either of the NMR

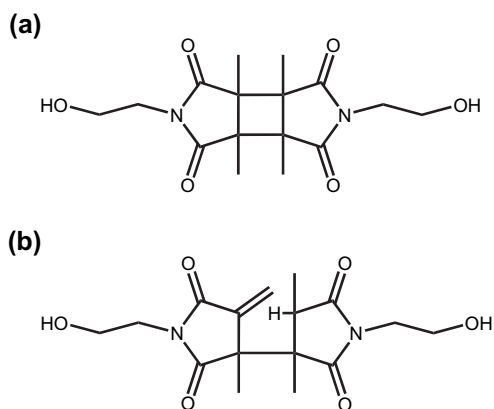


Fig. 5. Structures of dimers formed in TXS-sensitized photodimerization of HE-DMMI in aqueous solution: (a) precipitate and (b) dissolved product.

spectra, indicating that the dimerization reaction is complete after sufficient irradiation time.

A rerun of the reaction in D_2O as solvent showed no isotopic effect on results. This proves that the H-shift is occurring within the intermediate dimer complex. According to the Hammond model, this kind of process can be allocated to the T_1 excited dimer that has a wide geometry and is therefore prone to undergo side reactions before returning to the ground state S_0 . In several other photochemical homo- and heterocycloaddition reactions [78–80], similar behavior was observed and explained on the basis of H-shifts in an intermediate triplet excimer.

Employing different model compounds such as *N*-(2-aminoethyl)-dimethylmaleimide and *N*-(*N'*-acetyl-2-aminoethyl)-dimethylmaleimide in the photodimerization process in an aqueous medium gave results similar to those obtained with HE-DMMI. There was no precipitate appearing, but the NMR spectra of the products isolated from solution showed that they were mixtures of the corresponding asymmetric and symmetric dimers with the asymmetric compound appearing in large excess. These observations show that the formation of the asymmetric dimer is favored when the photodimerization proceeds in aqueous solution, while only unpolar media seem to favor the formation of the symmetric cyclobutane derivative. In either case, however, there is a 100% formation of dimers. This means that the photoreaction can be used to crosslink accordingly functionalized polymers, although the chemical structures of the crosslinks generated are different.

To ensure that the dimerization of the DMMI moieties is the only reaction occurring in the polymer system upon irradiation, the model reaction was repeated in the presence of acetamide, regarded to represent PAAm functionalities. There have been some reports suggesting that amide groups can undergo Paterno-Büchi analogous reactions [81] or photocleavage followed by subsequent interconnection processes. However, our experiments did not show any evidence for such side reactions. While the two isomeric dimers were detected in comparable ratio as in the last experiment, the NMR signals of acetamide were found to be unchanged in the mixture. Additionally, mass spectra showed no peaks that could be addressed to hetero-addition products (e.g., no peak at $m/z = 228$ that might be interpreted as the M^+ peak of an HE-DMMI–AcNH₂ adduct). Hence, unwanted side reactions do not occur to an extent exceeding the analytical sensitivity. There was also no evidence for further reactions of the DMMI dimers, even though most of them carry olefinic bonds.

4.2. Photoinduced crosslinking of *P*(AAm-co-DMMIAAm)

4.2.1. UV-vis analysis

We exemplify the UV-spectroscopic analysis of the progress of crosslinking by considering a semi-dilute solution of the sample PAAm–DMMI.5 (conc. 50 g L^{-1}) containing 10 mol% TXS, relating to the concentration of DMMI

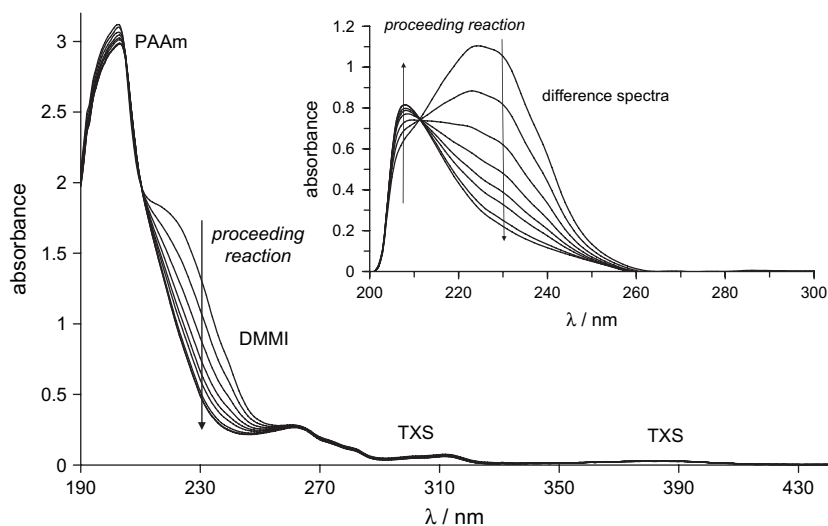


Fig. 6. UV–vis spectra recorded during crosslinking of a system of 50 g L^{-1} PAAm–DMMI1.5 in aqueous solution containing 10% TXS, related to the amount of DMMI moieties, at irradiation times of 0, 10, 20, 30, 40, 50, 70, 90 and 150 min. The inset shows the corresponding difference spectra obtained after subtraction of separately recorded and suitably scaled spectra of pure PAAm and TXS.

moieties. Fig. 6 shows the UV spectra recorded after several periods of irradiation. There is a shoulder at around 230 nm that decreases with irradiation time and that can be assigned to the DMMI moieties. It is superimposed on a strong background resulting from PAAm. Also recognized, albeit weak, are the absorption bands of TXS at 270, 310, and 380 nm, whereby the latter band is used for the initiation of the photo-reaction. By subtraction of separately recorded spectra of pure sensitizer and PAAm solutions that were scaled to coincide with the composite spectrum in the regions of 382 nm (sensitizer) and 201 nm (PAAm), the signal of the DMMI side groups and their dimers could be extracted, as depicted in the inset of Fig. 6. Obviously, there is a strong similarity to the spectra obtained for the reaction of the low molecular weight model compounds shown in Fig. 4: the signal of the original DMMI moieties at 229 nm decreases, while the band at 205 nm due to the dimeric products is enhanced. Again, all spectra intercept within an isosbestic point at 209 nm and therefore are linear combinations of the spectra of the pure reactants and their dimeric products, corresponding to $t = 0$ and $t = \infty$, respectively. The conversion of the reaction, $y(t)$, can be obtained via

$$y(t) = (A(t) - A(0)) / (A(\infty) - A(0)), \quad (1)$$

where $A(t)$ denotes the absorbance at time t , with $A(0)$ and $A(\infty)$ being the initial and final values. In principle, Eq. (1) holds for every wavelength, but $\lambda = 229 \text{ nm}$ (maximum of DMMI absorption) is used expediently because the absorption change is strongest at this wavelength.

To check for the accuracy and reproducibility of this spectroscopic procedure, two experiments were performed in parallel on the dimerization of the model compound HE-DMMI (8 mmol L^{-1} in aqueous solution containing 1 mmol L^{-1} TXS), where one solution contained only reactant and sensitizer, while the other one was supplemented with 50 g L^{-1}

PAAm in addition. The strong background absorbance of PAAm did not impair the analysis perceptibly, and identical conversion data were obtained within $\pm 1\%$.

As a further check, spectra were recorded on aqueous solutions of 20, 40, 60 and 80 g L^{-1} of the polymer sample PAAm–DMMI2.0 and 1 mmol L^{-1} TXS in 0.1 mm cuvettes. Spectra were also recorded on the fully crosslinked samples after extensive irradiation. Fig. 7 shows the absorbances of the DMMI moieties at $\lambda = 229 \text{ nm}$ that were separated from the composite spectra in the manner described above, as a function of the initial concentration of pendent DMMI groups. The results indicate excellent proportionality even at high concentrations, where the amount of DMMI is leading to differential absorbances exceeding 2 (for the unreacted solution) and the background absorbance due to polymer is high. The two lines are well represented by $A(0) = 14\,800 \text{ L (mol cm)}^{-1} c_{\text{DMMI}}$ and $A(\infty) = 3460 \text{ L (mol cm)}^{-1} c_{\text{DMMI}}$, respectively.

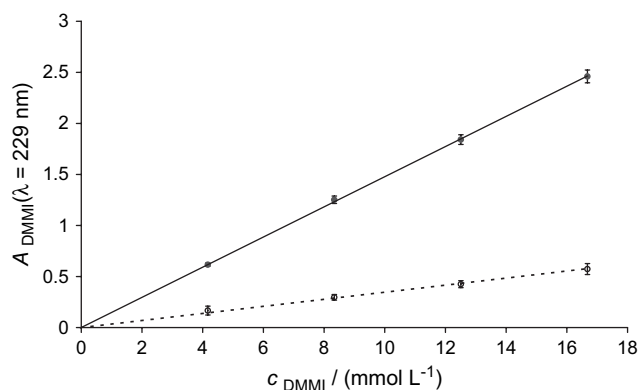


Fig. 7. Background-corrected absorbances at 229 nm of aqueous PAAm–DMMI2.0 solutions at concentrations of 20, 40, 60, and 80 g L^{-1} before (full circles, full line) and after complete crosslinking (open circles, dotted line) in 0.1 mm quartz cuvettes.

4.2.2. Influence of the amount of sensitizer and light dose on gelation kinetics

DMMI conversion, $y(t)$, was determined as a function of irradiation time for solutions containing the same amount of polymer (50 g L^{-1} PAAm–DMMI1.5) and variable quantities of sensitizer, ranging from 1 to 100% relating to the concentration of DMMI moieties. For one series, the incident light was made rather monochromatic ($\lambda = 383 \text{ nm}$) by using the interference filter, while for a second series the broad-band pass filter was applied ($\lambda > 310 \text{ nm}$) and the intensity was higher. From each course of conversion versus time, the half-life, τ , was determined. Fig. 8a shows a plot of $1/\tau$ versus the relative concentration of sensitizer. The data points for each series of measurements fall approximately on a straight line passing through the origin. This indicates that the rate of reaction is proportional to the concentration of sensitizer within experimental uncertainty. Perceptible deviations only occur at the highest TXS concentrations. The slopes of the two lines depicted are in a ratio of 1:10. The overlap integrals between the absorption band of TXS having its maximum at 382 nm and the transmittance curves of the filters (cf. Fig. 3) are estimated to be in a ratio of 1:12, which is in reasonably close

agreement. Hence, the rate of reaction is also roughly proportional to the intensity of light which can be absorbed by the sensitizer.

To check the second point in a more systematic way, Fig. 8b shows reciprocal half-lives versus relative light intensity for one selected composition (50 g L^{-1} PAAm–DMMI1.5, 100% TXS). The attenuation of intensity was achieved by using filter cascades. Although the number of data points is limited, it becomes obvious that $1/\tau$ is proportional to intensity.

These results demonstrate clearly that the crosslinking reaction can be well controlled by adjusting the amount of sensitizer and the intensity of irradiation. The rate of DMMI conversion is proportional to either of these two parameters. This means that the quantity of dimers (crosslinks) formed is directly related to the light dose absorbed by TXS molecules. Within the parameter space covered by our experiments, the transfer of energy from the excited sensitizer to the DMMI moieties, resulting in the formation of dimers, is occurring with constant efficiency.

Because of this simple dependency, it is possible to reduce the concentration of sensitizer and increase the duration and/or intensity of irradiation in return, in order to achieve identical conversion. This is particularly necessary when the layer thickness becomes large. The concentration of sensitizer then has to be adjusted to ensure sufficient transmittance through the sample layer to avoid formation of a gradient (e.g., in the NMR experiments).

Two additional observations need to be mentioned: none of the large number of UV spectra that were collected in the context of the present work showed any evidence for photobleaching of TXS. The corresponding absorption bands remained equally strong even when very high illumination intensities were utilized (e.g., in rheology under UV exposure, cf. next chapter). Also, there was no evidence for oxygen-quenching within the systems studied. Kinetic experiments conducted on nitrogen-flushed samples and on samples under air gave identical results. These facts demonstrate that the TXS-sensitized photoreaction is rather robust.

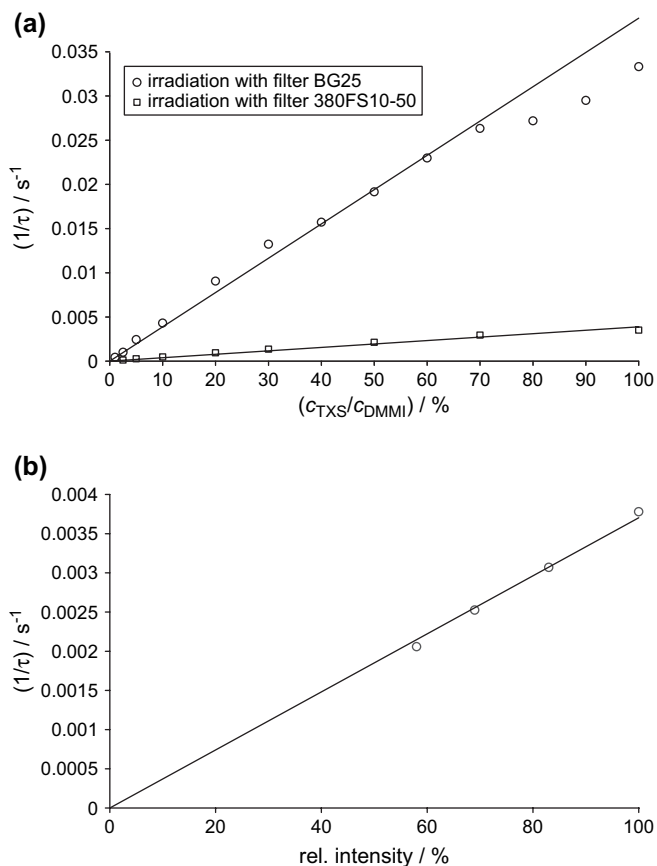


Fig. 8. Influence of (a) the amount of sensitizer and (b) irradiation intensity on the half-life of DMMI dimerization in a 50 g L^{-1} solution of PAAm–DMMI1.5 in water. Linear fits in (a) are represented by $(1/\tau)_{\text{BG25}} = 3.9 \times 10^{-4} \text{ s}^{-1} (c_{\text{TXS}}/c_{\text{DMMI}})/\%$ and $(1/\tau)_{\text{380FS10-50}} = 3.9 \times 10^{-5} \text{ s}^{-1} (c_{\text{TXS}}/c_{\text{DMMI}})/\%$. In (b), the molar concentration of TXS was identical to that of DMMI groups. The linear fit herein is represented by $(1/\tau) = 3.7 \times 10^{-5} \text{ s}^{-1} I_{\text{rel}}/\%$.

4.3. Rheological characterization of the gelation process

The oscillatory shear modulus was measured during the photochemically induced gelation process on samples containing PAAm–DMMI2.0 at concentrations of 20, 40, 60, and 80 g L^{-1} , as well as 1 mmol L^{-1} of TXS. Note that the UV irradiation in these runs was considerably more intense than in the other experiments (cf. Section 3.6).

The equilibrium (zero frequency) shear modulus, G , is related to the effective network density of a gel, ν_{eff} , by:

$$G = f\nu_{\text{eff}}RT, \quad (2)$$

where f is a structure factor, which can be equated to 1/2 in the case of tetrafunctional crosslinks in swollen networks. ν_{eff} is the molar number of network strands per volume, which is twice the molar number of crosslinks per volume. The quantity actually measured was the storage modulus G' (4 Hz), and also

the corresponding loss modulus, G'' (4 Hz). If $G' > G''$, the storage modulus is close to the equilibrium modulus and can be used to estimate ν_{eff} .

Fig. 9 shows the temporal course of G' for a 60 g L^{-1} semi-dilute sample of PAAm–DMMI2.0 during irradiation. Initially, we have a polymer solution, and the finite storage modulus reflects the temporal entanglement network. Shortly after the onset of irradiation, G' rises steeply and finally approaches a plateau value. (G'' is remaining below 50 Pa throughout the experiment.) This course is due to the formation of the permanent network structure via dimerization of the DMMI moieties. To compare the conversion of DMMI moieties with the rise of G' , the chemical conversion in samples irradiated under exactly identical conditions for some selected irradiation periods was determined by UV–vis spectroscopy and plotted in the same graph. The development of both quantities occurs in a strictly parallel manner. Hence, the formation of elastically effective crosslinks is proportional to the DMMI conversion.

The plateau values of G' for the whole series of experiments are listed in Table 2 together with other characteristic data. From G' , the effective network density, ν_{eff} , was determined, while the molar concentration of DMMI moieties equals the theoretical network density, ν_{th} . The ratio of the two, $\nu_{\text{eff}}/\nu_{\text{th}}$, is thus a measure of crosslinking efficiency. The results in Table 2 show that the efficiency is around 16% at low polymer concentration, presumably because most dimerizations are formed intramolecularly, but rises distinctly with rising concentration up to more than 60% for the 80 g L^{-1} system. The crosslinking efficiency achieved with this photochemical procedure is therefore by far greater than that observed when polyacrylamide gels are made by crosslinking copolymerization [7].

4.4. Characterization of the network structures by multiple-quantum NMR

4.4.1. Basic principles of proton NMR of networks

In general, the proton line shape, or, equivalently, the transverse relaxation behavior of the proton NMR signal of

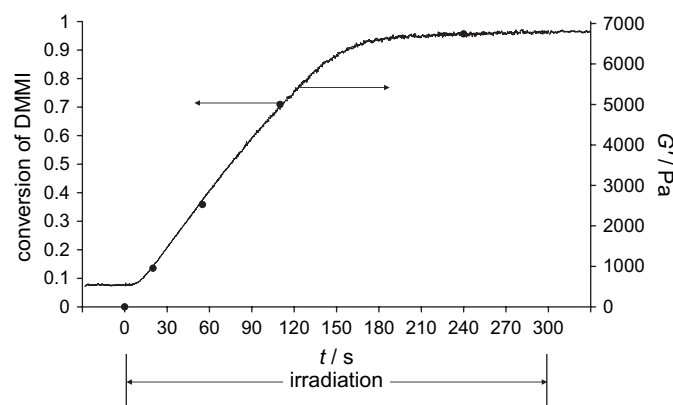


Fig. 9. Temporal course of G' measured by rheology under UV exposure (continuous line) and conversion of pendent DMMI groups measured by UV–vis spectroscopy (full circles) for an aqueous 60 g L^{-1} semi-dilute sample of PAAm–DMMI2.0 with 1 mmol L^{-1} TXS.

Table 2

Plateau values of G' (4 Hz) in the fully crosslinked state of semi-dilute PAAm–DMMI2.0 hydrogels and crosslinking efficiencies derived thereof

$c_{\text{PAAm-DMMI2.0}}$ (g L^{-1})	$c_{\text{DMMI}} = \nu_{\text{th}}$ (mmol L^{-1})	G' (Pa)	ν_{eff} (mmol L^{-1})	Efficiency of crosslinking $\nu_{\text{eff}}/\nu_{\text{th}}$ (%)
20	4.17	815	0.66	15.8
40	8.34	2092	1.69	20.2
60	12.51	6730	5.43	43.4
80	16.68	12835	10.36	62.1

polymers or networks far above their glass transition temperature or in the swollen state, reflects the timescale of the chain dynamics and also the presence of restrictions to the dynamics, i.e., the presence of crosslinks. Isotropically mobile, unconnected chains (e.g., sol), which fluctuate rapidly, contribute a slowly relaxing component (narrow line), while network chains fluctuate slightly anisotropically due to the constraints imposed by the crosslinks, and thus exhibit a significantly faster relaxation (broader line). Therefore, the different components of a swollen network can be differentiated.

The reason for the broader lines of network chains is ultimately related to the fact that their NMR response is partially solid-like, i.e., dipolar interactions are only incompletely averaged out. Note that in solids, strong dipolar interactions lead to very broad lines, while they are totally averaged out in the case of isotropically mobile liquids. The presence of crosslink-induced *residual dipolar couplings* (D_{res}) in a network (a “soft” solid) leads to the accelerated relaxation behavior as compared to a normal liquid. Theory shows that the magnitude of the residual dipolar coupling is inversely proportional to the chain length between the crosslinks and thus directly proportional to the crosslink density [76,82]. Its precise measurement is therefore highly worthwhile. Technically speaking, the intensity decay process in a relaxation experiment is in this case due to coherent spin evolution (dipolar dephasing) rather than “real” fast-motion-induced relaxation. Since true relaxation processes always act simultaneously with the dipolar dephasing, making analyses of relaxation curves model-dependent, it is advantageous to *directly* measure the residual dipolar couplings in an experiment where their presence leads to a quantifiable intensity *build-up* rather than a decay. In this respect, multiple-quantum (MQ) NMR has evolved as one of the most quantitative approaches, as not only absolute values of D_{res} , but also its distribution can be measured [74–76,83,84].

4.4.2. Analysis of the MQ NMR data: component separation

The MQ NMR experiment yields a double-quantum intensity, $I_{\text{DQ}}(\tau_{\text{DQ}})$, that is dependent on the product of the residual dipolar coupling and the evolution time, τ_{DQ} , under a specific MQ pulse sequence. In a concurrent experiment (that differs in the so-called phase cycle of the receiver), a reference intensity, $I_{\text{ref}}(\tau_{\text{DQ}})$, is measured, which belongs to that part of the total magnetization that has not yet evolved into double-quantum coherences. It contains a complementary contribution from dipolar coupling modulated magnetization of the network (a part of the dipolar spin evolution process), and also all

contributions from more mobile non-network components. It should be mentioned that the experiments were conducted on a low-field instrument, where both intensities can be determined from an average over the initial 100 μs of the featureless FID after a 90° pulse that follows the actual MQ pulse sequence, during which time the signal did not decay appreciably [75].

The sum of DQ and reference intensities, $I_{\Sigma\text{MQ}} = I_{\text{DQ}}(\tau_{\text{DQ}}) + I_{\text{ref}}(\tau_{\text{DQ}})$, was normalized according to $I_{\Sigma\text{MQ}}(\tau_{\text{DQ}} = 0) = 1$. Then, a contribution termed C-fraction could be separated by fitting the long-time tail of the decaying function to a single exponential with initial amplitude f_C and relaxation time τ_C . The C-fraction corresponds to very mobile components such as solvent and sol that have the longest relaxation time. It is not of major interest here and was subtracted from $I_{\Sigma\text{MQ}}$.

A second contribution (B) that is polymeric in nature but elastically inactive and can be associated with dangling chains, loops and related structures, has to be subtracted as well, for instance in a way described earlier (e.g., Ref. [83]). The reliable fitting of this second contribution, which also decays approximately exponentially, was in our case challenged by the fact that the corresponding relaxation time τ_B is very close to the relaxation time of the $I_{\Sigma\text{MQ}}(\tau_{\text{DQ}})$ intensity of the pure network component (A) under the given conditions, even though this component is not network-like and does not contribute to the DQ intensity build-up. This is so because the ultimately isotropic segmental motions of this component occur on a timescale that is similar to that of the network chains, as opposed to the faster and isotropically mobile sol part C. In this case, an alternative approach had to be taken that makes use of the fact that the final DQ intensity of the network part has to evolve to the same level as the corrected reference intensity, i.e., $I_{\text{DQ}}/I_{\Sigma\text{MQ,corr}} \equiv I_{n\text{DQ}} = 0.5$ as $\tau_{\text{DQ}} \rightarrow \infty$ [76,83,85]. This condition was met by multiplying the C-corrected sum intensity $I_{\Sigma\text{MQ}}(\tau_{\text{DQ}})$ by a constant factor, $1 - f_B$, chosen such that the so-called normalized DQ build-up curve, $I_{n\text{DQ}}(\tau_{\text{DQ}})$, approaches the theoretically expected value of 0.5 in its long-time limit. The contribution of effective network chains (A) to the total signal intensity is then simply given by $f_A = 1 - f_B - f_C$. It should be noted that several experiments conducted at 80°C yielded the same results for the different fractions within experimental accuracy. However, the relaxation times τ_A and τ_B were then different such that the B-component could be extracted by direct tail fitting.

Table 3 shows a listing of the fractions of the three components A, B, and C as well as their apparent relaxation times at 25°C . τ_C values are in the range of several hundred ms, while the common $\tau_A = \tau_B$ is around 10 ms. Besides a roughly constant portion of about 20% sol and solvent in all samples, f_A is distinctly increasing with rising polymer concentration on the expense of f_B . This is another indication of the fact that the higher the polymer concentration, the more is the formation of elastically effective crosslinks favored over the formation of intramolecular linkages leading to loops, etc. f_A is thus considered a measure of crosslinking efficiency and complements and confirms nicely the results obtained by rheology (cf.

Table 3

Results of MQ NMR experiments on semi-dilute samples of PAAm–DMMI.0 in the fully crosslinked state (solvent: D_2O)

$c_{\text{PAAm–DMMI.0}}$ (g L^{-1})	f_A (%)	f_B (%)	f_C (%)	$\tau_{A,B}$ (ms)	τ_C (ms)	D_{res} (Hz)
20	11.5	56.5	32.0	14.2	1369.9	85.1
40	32.4	48.6	19.0	11.1	404.9	109.6
60	40.4	40.4	19.2	10.4	423.7	128.9
80	44.0	31.8	24.2	8.9	251.9	127.2

f_A, f_B , and f_C are the fractions of network chains, dangling chains etc., and sol, respectively, τ_A, τ_B , and τ_C are the corresponding relaxation times, and D_{res} is the residual dipolar coupling parameter. All data correspond to $T = 25^\circ\text{C}$.

Table 2). Note that rheological and MQ NMR measurements were performed on PAAm samples which differ in DMMI content by a factor of about 2. This shows that the amount of dimerizable moieties within the precursor chains has only a minor effect on the relative amount of elastically effective junctions formed, while the influence of polymer concentration is much more significant.

4.4.3. Analysis of the network fraction

Fig. 10 shows the DQ build-up curves of the network component in the gel samples studied, obtained after appropriate normalization as just described. The build-up of $I_{n\text{DQ}}$ with τ_{DQ} depends on the residual dipolar coupling constant, D_{res} , in the following way:

$$I_{n\text{DQ}}(D_{\text{res}}) = \frac{1}{2} \left(1 - \exp \left\{ -\frac{2}{5} D_{\text{res}}^2 \tau_{\text{DQ}}^2 \right\} \right) \quad (3)$$

D_{res} in turn is, as mentioned above, inversely related to the apparent chain length between restrictions [74,82,84]. In general, a distribution of chain lengths and, hence, a distribution of coupling constants needs to be considered. For the evaluation of our data, a gamma distribution was assumed as discussed in detail in Ref. [76]. It is ideally expected in a system with fixed

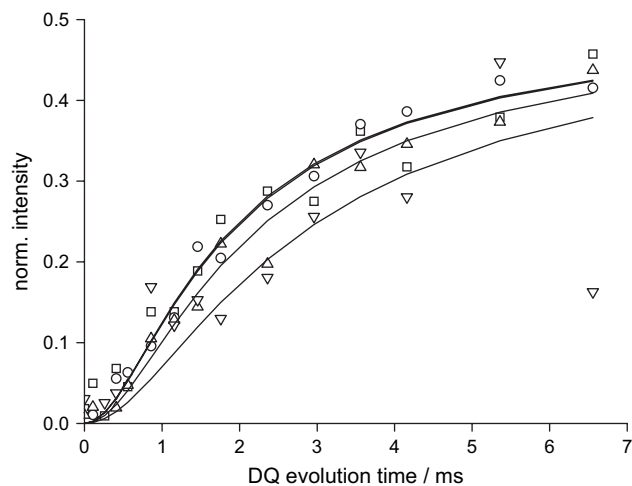


Fig. 10. Normalized DQ build-up curves obtained from MQ NMR characterization of semi-dilute PAAm–DMMI.0 samples in their fully crosslinked states at concentrations of 20 (∇), 40 (\triangle), 60 (\circ), and 80 g L^{-1} (\square) in D_2O .

chain length between crosslinks and a Gaussian distribution of end-to-end distances.

$$P(|D_{\text{res}}|) = \frac{2}{\sqrt{\pi}} \sqrt{\frac{27|D_{\text{res}}|}{8D_{\text{res}}^3}} e^{-3|D_{\text{res}}|/(2\bar{D}_{\text{res}})} \quad (4)$$

The experimental $I_{n\text{DQ}}(\tau_{\text{DQ}})$ data were then fitted in the region of $I_{n\text{DQ}} < 0.45$ by numerically integrating over the entire range of $D_{\text{res}} = 0 \dots \infty$ to give a mean value of a relatively broad distribution (the width of a gamma distribution depends on its average, whereby no additional fitting parameter is introduced). Results of these fits are shown in Fig. 10 as full lines, and the average coupling constants are included in Table 3.

The coupling constants and the courses of $I_{n\text{DQ}}(\tau_{\text{DQ}})$, respectively, are quite similar for all PAAm–DMMI gels in this series, despite of different concentrations and crosslinking efficiencies. This indicates that the mean lengths of active network chains are similar, and a consideration of the crosslinking mechanism can explain this finding: a linkage between two polymer chains is only formed upon dimerization of two DMMI side groups and, therefore, the chain length between crosslinks (and its distribution) is essentially predetermined by the given random spacing of DMMI moieties along the initial polymer chains. Of course, this argument holds only when conversion is complete.

The experimental finding also implies that dimerizations which are not generating elastically active network chains are not leading to chain extension to any appreciable extent. This is a surprising and important observation in view of the marked variation of the A fraction determined by MQ NMR or the crosslinking efficiency, respectively, with polymer concentration. The necessity to assume a broad distribution of coupling constants according to Eq. (4) to attain reasonable fitting of the build-up curves is in accord with previous observations on swollen networks [85]. While distributions due to variations in the chain length between crosslinks as well as the distribution expected on the basis of a Gaussian distribution of end-to-end distances are screened by the cooperativity of the chain motions (“packing”) in unswollen elastomers, such effects, as well as topologically induced swelling heterogeneities, reappear in swollen networks [76,85,86].

5. Conclusions

Photochemical crosslinking of DMMI-functionalized PAAm provides an efficient way to synthesize hydrogels in a selective and controlled manner. We have shown that the photodimerization of DMMI moieties in aqueous solution yields predominantly asymmetric products instead of the initially expected cyclobutane derivatives, known from the reaction in organic solvents. However, the dimerization reaction occurs without perceptible side reactions and can be readily controlled by the intensity and duration of UV irradiation and the concentration of sensitizer. It is therefore very well suited to crosslink a polymer solution at will if the initial polymer is equipped with such functional groups. The gelation process can be

interrupted at any stage by discontinuing the UV irradiation in order to study the system as it changes from a semi-dilute polymer solution to a fully crosslinked gel.

The conversion of DMMI moieties into dimers is easily quantified by UV spectroscopy. Since not all such chemical linkages are elastically effective, methods to determine the crosslinking efficiency were applied. On a macroscopic scale, the rheological measurement of the shear modulus is a measure for the density of effective network chains. Comparison with the amount of dimerized DMMI units shows that the crosslinking efficiency is around 16% when a solution containing 20 g L^{-1} of functionalized polymer is crosslinked, and rises to more than 60% at a concentration of 80 g L^{-1} . These efficiencies are surprisingly high in view of the fairly small concentrations and markedly exceed the values typically attained when gelation occurred by crosslinking copolymerization of monomer and crosslinker.

The macroscopic determination of crosslinking efficiency is supported by MQ NMR experiments yielding information on the fraction of monomer units present in elastically effective network chains. Quantification of these, becoming possible because of the residual dipolar coupling between such units, gave values comparable to the ones obtained by rheology. Furthermore, the MQ NMR measurements indicate that the average length of active network chains is just slightly dependent on crosslinking efficiency or concentration, a fact that can be traced back to the importance of the spacing of functional groups along the initial polymer chains. Hence, the results of spectroscopic analysis, rheology and MQ NMR experiments produce a consistent picture of PAAm network formation through sensitized photodimerization of pendent DMMI groups.

Acknowledgements

We thank Jan C. Namyslo and the NMR group of the Institute of Organic Chemistry, Clausthal University of Technology, for performing the high resolution NMR measurements (Sections 3.1–3.4), as well as Tobias Habeck for recording the mass spectra. Furthermore, Leonore Schwegler and Petra Kuschel from Bosch AG, Gerlingen, Germany, are gratefully acknowledged for providing the possibility to perform rheological measurements under UV exposure.

Financial support for this study from the Deutsche Forschungsgemeinschaft is gratefully acknowledged.

References

- [1] Thomas WM. Acrylamide polymers. In: Bikales NM, editor. Encyclopedia of polymer science and technology, vol. 1. New York: Wiley; 1964.
- [2] Montgomery WH. Polyacrylamide. In: Davidson RL, Sittig M, editors. Water-soluble resins. 2nd ed. New York: Van Nostrand Reinhold; 1968.
- [3] Bikales NM. In: Bikales NM, editor. Water soluble polymers. Polymer science and technology, vol. 2. New York: Plenum; 1973.
- [4] Molyneux P. Water-soluble synthetic polymers: properties and behavior. Boca Raton, Florida: CRC Press; 1984.
- [5] White ML. J Phys Chem 1960;64:1563.

- [6] Mallam S, Horkay F, Hecht AM, Geissler E. *Macromolecules* 1989;22:3356.
- [7] Lindemann B, Schröder UP, Oppermann W. *Macromolecules* 1997;30:4073.
- [8] Kizilay MY, Okay O. *Macromolecules* 2003;36:6856.
- [9] Ichimura K, Watanabe S. *J Polym Sci Polym Chem Ed* 1982;20:1419.
- [10] Ichimura K. *J Polym Sci Polym Chem Ed* 1984;22:2817.
- [11] Shindo Y, Katagiri N, Ebisuno T, Hasegawa T, Mitsuda M. *Angew Makromol Chem* 1996;240:231.
- [12] Cockburn ES, Davidson RS, Pratt JE. *J Photochem Photobiol A* 1996;94:83.
- [13] Schinner R, Wolff T, Kuckling D. *Ber Bunsen-Ges Phys Chem* 1998;102:1710.
- [14] Farnum DG, Mostashari AJ. *Org Photochem Synth* 1971;1:103.
- [15] Cohen MD, Schmidt JMG. *J Chem Soc* 1964;1996.
- [16] Rennert J, Ruggiero EM, Rapp J. *Photochem Photobiol* 1967;6:29.
- [17] Rennert J. *Photogr Sci Eng* 1971;15:60.
- [18] Tsuda M. *J Chem Soc Jpn* 1969;42:905.
- [19] Oikawa S, Tsuda M, Ueno N, Sugita K. *Chem Phys Lett* 1980;74:379.
- [20] Tsuda M. *J Polym Sci A* 1964;2:2907.
- [21] Egerton PL, Pitts E, Reiser A. *Macromolecules* 1981;14:95.
- [22] Nakayama Y, Matsuda T. *J Polym Sci A* 1992;30:2451.
- [23] Minsk LM, Smith IG, Wright JF. *J Appl Polym Sci* 1959;2:302.
- [24] Robertson EM, Van Deusen WP, Minsk LM. *J Appl Polym Sci* 1959;2:308.
- [25] Coqueret X. *Macromol Chem Phys* 1999;200:1567.
- [26] Williams JLR, Farid SY, Doty JC, Daly RC, Specht DP, Searle R, et al. *Pure Appl Chem* 1977;49:523.
- [27] Williams JLR. *Fortschr Chem Forsch* 1969;13:227.
- [28] Schenck GO, von Wilucki I, Krauch CH. *Chem Ber* 1962;95:1409.
- [29] Krauch CH, Farid S, Schenck GO. *Chem Ber* 1966;99:625.
- [30] Hammond GS, Stout CA, Lamola AA. *J Am Chem Soc* 1964;86:3103.
- [31] Kuznetsova NA, Kaliya OL. *Russ Chem Rev* 1992;61:683.
- [32] Chujo Y, Sada K, Saegusa T. *Macromolecules* 1990;23:2693.
- [33] Ngai T, Wu C. *Macromolecules* 2003;36:848.
- [34] Schenck GO, Hartmann W, Mannsfeld SP, Metzner W, Krauch CH. *Chem Ber* 1962;95:1642.
- [35] De Schryver FC, Bhardwai I, Put J. *Angew Chem* 1969;81:224.
- [36] De Schryver FC, Feast WJ, Smets G. *J Polym Sci A-1* 1970;8:1939.
- [37] De Schryver FC, Boens N, Smets G. *J Polym Sci A-1* 1972;10:1687.
- [38] Put J, De Schryver FC. *J Am Chem Soc* 1973;95:137.
- [39] Zweifel H. *Photogr Sci Eng* 1983;27:114.
- [40] Berger J, Zweifel H. *Angew Makromol Chem* 1983;115:163.
- [41] Finter J, Widmer E, Zweifel H. *Angew Makromol Chem* 1984;128:71.
- [42] Finter J, Haniotis Z, Lohse F, Meier K, Zweifel H. *Angew Makromol Chem* 1985;133:147.
- [43] Decker C, Bianchi C. *Polym Int* 2003;52:722.
- [44] Ling L, Habicher WD, Kuckling D, Adler HJP. *Des Monomers Polym* 1999;2:351.
- [45] Kuckling D, Adler HJP, Ling L, Habicher WD, Arndt KF. *Polym Bull* 2000;44:268.
- [46] Duan Vo C, Kuckling D, Adler HJP, Schönhoff M. *Colloid Polym Sci* 2002;280:400.
- [47] Kuckling D, Duan Vo C, Wohrab SE. *Langmuir* 2002;18:4263.
- [48] Kuckling D, Duan Vo C, Adler HJP, Völkel A, Cölfen H. *Macromolecules* 2006;39:1585.
- [49] Roth M, Muller B. *Polym Paint Col J* 1988;178:209.
- [50] Herkstroeter WG, Lamola AA, Hammond GS. *J Am Chem Soc* 1964;86:4537.
- [51] Hammond GS, Turro NJ, Leermakers PA. *J Phys Chem* 1962;66:1144.
- [52] Wilkinson F. *J Phys Chem* 1962;66:2569.
- [53] Steinmetz R. *Fortschr Chem Forsch* 1967;7:445.
- [54] Scharf HD. *Fortschr Chem Forsch* 1969;11:216.
- [55] Murov SL. *Handbook of photochemistry*. New York: Marcel Dekker Inc.; 1973.
- [56] Schenck GO, Steinmetz R. *Bull Soc Chim Belg* 1962;71:78.
- [57] Engel PS, Monroe BM. *Adv Photochem* 1972;8:245.
- [58] Lathioor EC, Leigh WJ. *Photochem Photobiol* 2006;82:291.
- [59] Kronfeld KP, Timpe HJ. *J Prakt Chem* 1988;330:571.
- [60] Ferreira GC, Schmitt CC, Neumann MG. *J Braz Chem Soc* 2006;17:905.
- [61] Green WA, Timms AW. *Photoinitiating systems*. In: Fouassier JP, Rabek I, editors. *Radiation curing in polymer science and technology*, vol. 2. UK: Elsevier; 1993.
- [62] Fouassier JP. *Photoinitiation, photopolymerization and photocuring*. Cincinnati: Hanser Gardner; 1995.
- [63] Allonas X, Ley C, Bibaut C, Jacques P, Fouassier JP. *Chem Phys Lett* 2000;322:483.
- [64] Lewis FD, Saunders WH. *J Am Chem Soc* 1968;90:7033.
- [65] Krystkowiak E, Maciejewski A, Kubicki J. *ChemPhysChem* 2006;7:597.
- [66] Meier K, Zweifel H. *J Photochem* 1986;35:353.
- [67] Gupta A, Mukhtar R, Seltzer S. *J Phys Chem* 1990;84:2356.
- [68] Fevola MJ, Hester RD, McCormick CL. *J Polym Sci A* 2003;41:560.
- [69] Pabon M, Selb J, Candau F, Gilbert RG. *Polymer* 1999;40:3101.
- [70] Tanaka T. *Sci Am* 1981;244:124.
- [71] Gupta MK, Bansil R. *Polym Prepr (Am Chem Soc Div Polym Chem)* 1981;22:375.
- [72] Gottlieb HE, Kotlyar V, Nudelman A. *J Org Chem* 1997;62:7512.
- [73] McCarthy KJ, Burkhardt CW, Parazak DP. *J Appl Polym Sci* 1987;33:1699.
- [74] Saalwächter K, Ziegler P, Spycykerelle O, Haidar B, Vidal A, Sommer JU. *J Chem Phys* 2003;119:3468.
- [75] Saalwächter K, Gottlieb M, Liu R, Oppermann W. *Macromolecules* 2007;40:1555.
- [76] Saalwächter K. *Prog Nucl Magn Reson Spectrosc* 2007;51:1.
- [77] Bryce-Smith D, Bullen GJ, Clark NH, Connert BE, Gilbert A. *J Chem Soc C* 1966;167.
- [78] Mark G, Matthäus H, Mark F, Leitch J, Henneberg D, Schomburg G, et al. *Monatsh Chem* 1971;102:37.
- [79] Wexler AJ, Hyatt JA, Raynolds PW, Cottrell C, Swenton JS. *J Am Chem Soc* 1978;100:512.
- [80] Hanifin JW, Cohen E. *J Am Chem Soc* 1969;91:4494.
- [81] Tominaga T, Tsutsumi S. *Tetrahedron Lett* 1969;37:3175.
- [82] Cohen-Addad JP. *J Chem Phys* 1973;60:2440; Gottlieb YY, Lifshitz MI, Shevelev VA, Lishanskij IS, Balanina IV. *Vysokomol Soedin* 1976;A18(10):2299.
- [83] Saalwächter K, Klüppel M, Luo H, Schneider H. *Appl Magn Reson* 2004;27:401.
- [84] Saalwächter K, Herrero B, López-Manchado MA. *Macromolecules* 2005;38:9650.
- [85] Saalwächter K, Kleinschmidt F, Sommer JU. *Macromolecules* 2004;37:8556.
- [86] Saalwächter K, Sommer JU. *Macromol Rapid Commun* 2007;28:1455.